THE HYDRATION STATE OF CHLORIDE SALT DEPOSITS ON MARS. T. D. Glotch[1], B. P. Phillips[1], J. L. Bandfield[2], M. M. Osterloo[3], and A. D. Rogers[1], [1]Department of Geosciences, Stony Brook University, Stony Brook, NY 11794-2100 (timothy.glotch@stonybrook.edu, [2]Space Science Institute, Boise, ID, [3]University of Colorado, Boulder, CO.

Introduction: Chloride salt-bearing deposits on Mars were discovered using multispectral thermal infrared (TIR) imagery from the Thermal Emission Imaging System (THEMIS) [1]. Since then, these deposits have systematically been mapped and characterized using both TIR and visible/near-IR (VNIR) data sets [2-5]. Globally, the deposits occur throughout the southern highlands of Mars, primarily in Noachian terrains [6]. Light scattering models and laboratory spectra of chloride/silicate mixtures at both VNIR and TIR wavelengths suggest the Martian deposits are mixtures of an anhydrous chloride salt, such as halite, with the regional basaltic regolith. Salt abundances are estimated at 10-20 wt.%, suggesting deposition in a surficial and/or groundwater evaporative environment [7].

Unlike most terrestrial evaporite deposits, the Martian deposits do not appear to be associated with any other evaporite or alteration minerals (e.g., sulfates, carbonates, perchlorates, phyllosilicates, etc.). In some locations, most notably, Terra Sirenum, salt-bearing deposits are in close proximity to phyllosilicates, although geologic evidence suggests that they formed in separate events [3]. Both remote sensing [8] and laboratory work [9] are being conducted to further understand the nature of these deposits and the minimum percentage of other evaporite phases that could be present and still be consistent with the lack of absorption features in the Martian VNIR data sets.

In this work, we use data from the Compact Reconnaissance Imaging Spectrometer for Mars (CRISM) to characterize the hydration state of Martian salt-bearing deposits. CRISM ratio spectra of the salt deposits over the 1.0-2.5 μm region show no discernable 1.4 or 1.9 μm bands due to OH and H_2O. In addition, several authors have noted that the broad 3 μm band, also due to combinations of OH and H_2O modes, is much shallower over salt-bearing deposits than typical surrounding terrain [2-3]. These qualitative observations all suggest that Martian salt deposits are substantially desiccated compared to typical Martian regolith.

Milliken and Mustard [10] and Milliken et al. [11] provided the laboratory and theoretical framework for quantifying surface hydration based on remote sensing measurements of the 3 μm band in VNIR data sets. Through a series of carefully measured laboratory spectra of a variety of hydrated materials, they showed that a linear relationship exists between wt.% H_2O and Hapke's effective single particle absorption thickness (ESPAT) parameter measured at one of several specific wavelengths near 3 μm. As a preliminary investigation, we use this relationship described in [10] to quantify the hydration state of a Martian salt-bearing deposit in Terra Sirenum and compare it to the surrounding basaltic regolith.

Methods: CRISM images of interest are atmospherically corrected using the Discrete Ordinates Radiative Transfer (DISORT) model [12] according to the methods of [13]. The Martian surface is modeled as a Hapke scatterer, resulting in surface single scattering albedo spectra. Prior to atmospheric correction, the spectra are subjected to a simple temperature correction to account for the effects of thermal emission at wavelengths longer than ~3 μm. Subsequent to thermal and atmospheric correction, we perform a continuum removal over the 3 μm absorption band and convert to ESPAT according to :$ESPAT = \frac{1-w}{w}$.
where w is the single scattering albedo. We calculate wt.% H_2O from the 3.1 μm band minimum according to the relationship in [10]:$H_2O = 11.6270 * ESPAT$.

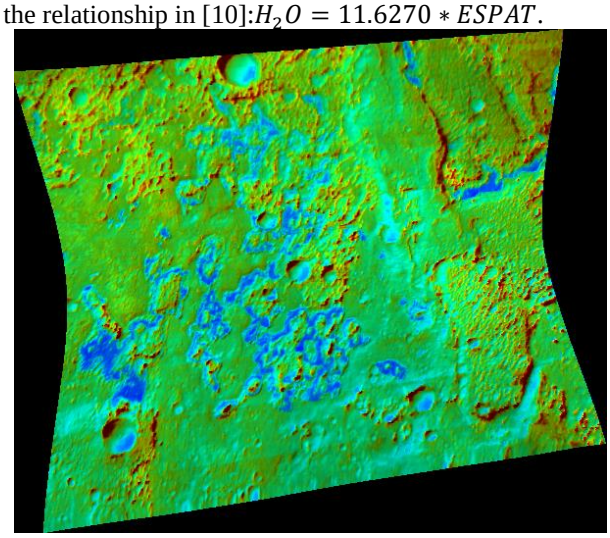

Figure 1. ESPAT parameter for FRTA253_0007 in Terra Sirenum overlayed on a single scattering albedo image at 1.3 μm. Absolute ESPAT values range from ~0.1 (blue) to ~0.55 (red). Blue regions correspond to chloride salt deposits and red regions correspond to hydrated Fe-Mg phyllosilicates.

Results: Figures 1 and 2 show the ESPAT parameter and wt.% H_2O content in FRT0000A253_07 derived at 3.14 μm. In both images, blue regions correspond to chloride salt-bearing deposits, and red regions correspond to Fe/Mg-bearing phyllosilicates [3]. Representative single scattering albedo spectra from

these regions, as well as the typical basaltic regolith are shown in Figure 3.

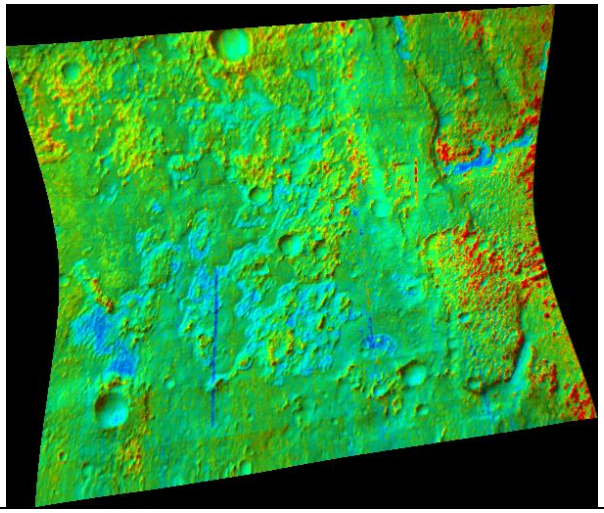

Figure 2. Derived wt.% H_2O for FRTA253_0007 in Terra Sirenum overlayed on a single scattering albedo image at 1.3 µm. Blue regions correspond to chloride salt deposits and red regions correspond to hydrated Fe-Mg phyllosilicates. Water abudances range from ~1% (blue) to ~10% (red).

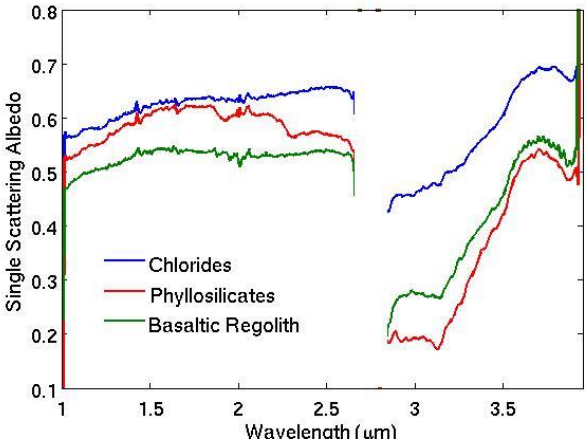

Figure 3. Representative single scattering albedo spectra from chloride-bearing deposits, phyllosilicate-bearing deposits, and typical basaltic regolith in FRTA253_07.

Chloride salt deposits in this image have derived water abundances of ~1 wt.%, while the phyllosilicate-bearing deposits have derived water abundances of ~10%. Typical basaltic regolith in this image has a derived water content of ~4 wt.%.

Discussion and Conclusions: Although the OMEGA-derived hydration maps of [11] did not cover much of the southern hemisphere of Mars, the water content we derived for the basaltic regolith in Terra Sirenum is consistent with typical Noachian highlands terrain mapped in that study. It is also broadly consistent with the Gamma Ray Spectrometer-derived water equivalent hydrogen for the region [14].

Several sources of uncertainty could affect the abshydration values derived in this work. Our model for atmospheric correction relies on several inputs, including estimates of dust and ice opacity, the atmospheric temperature/pressure profile, and surface roughness. Errors in these inputs would result in changes to the surface single scattering albedos, although changes to the 3 µm region would likely be minimal.

A likely larger source of error is the thermal correction employed in this work. For surface temperatures above ~280 K, thermal emission contributes substantially to the measured spectrum beyond ~3 µm. Warmer surface temperatures result in an upturn in the measured spectrum and a resulting decrease in the 3 µm band depth and derived water abundance. We utilize a simple thermal correction model that assumes a single surface temperature derived from the average albedo and thermal inertia for the entire scene. For relatively flat surfaces, the simple correction is likely valid. However for scenes with substantial topography and warm surfaces, the simple correction would underestimate and over-estimate the temperature correction for sun-facing and shadowed slopes, respectively. Future work will focus on testing the temperature correction over a variety of scenes and topographic regimes.

Martian chloride salt deposits investigated here appear to be highly desiccated relative to typical basaltic regolith and nearby phyllosilicate-bearing surfaces. Despite the potential sources of error, the derived water content of these deposits (~1 wt.%) appears quite low and precludes the presence of hydrous salts in large abundances. This is consistent with previous analyses that indicated that anhydrous chloride salts such as halite are responsible for the unique spectral signatures seen in both TIR and VNIR data sets. Any proposed formation mechanism for chloride salt deposits on Mars must be reconciled with their apparently desiccated nature and the absence of hydrated salts.

References: : [1] Osterloo, M. M. et al. (2010), JGR, 115. [2] Murchie, S. L. et al. (2009), *JGR*, 114, E00D06. [3] Glotch, T. D. et al. (2010), *GRL*, 37, L16202. [4] Osterloo, M. M. and B. M. Hynek (2015), *Geology*, 43, 787-790. [5] Ruesch, O. et al. (2012), JGR, 117, E00J13. [6] Osterloo, M. M. et al. (2010), *JGR*, 115, E10012. [7] Glotch, T. D. et al. (2016), *JGR*, 121, 454-471. [8] Phillips, B. P. et al. (2017), *Lunar Planet Sci. XLVIII*. [9] Ye, C., and T. D. Glotch (2017), *Lunar Planet. Sci. XLVIII*. [10] Milliken, R. E., and J. F. Mustard (2005), *JGR*, 110, E12001. [11] Milliken, R. E. et al. (2011), *JGR*, 112, 2156-2202. [12] Stamnes, K. S. et al. (1988), *Appl. Opt*., 27, 2502-2509. [13] Liu, Y. et al. (2016), *JGR*, 121, 2004-2036. [14] Feldman, W. C. et al. (2004), *JGR*, 109, E09006.